Environmental Pollution 317 (2023) 120766

Contents lists available at ScienceDirect

Environmental Pollution

journal homepage: www.elsevier.com/locate/envpol

Effects of benzo[a]pyrene on the reproductive axis: Impairment of kisspeptin signaling in human gonadotropin-releasing hormone primary neurons☆

Giulia Guarnieri [a], Matteo Becatti [b], Roberta Squecco [a], Paolo Comeglio [b], Rachele Garella [a], Lara Tamburrino [a], Sara Marchiani [a], Linda Vignozzi [b,c], Gabriella Barbara Vannelli [a], Mario Maggi [b,c], Annamaria Morelli [a,*]

[a] Department of Experimental and Clinical Medicine, University of Florence, Florence, Italy
[b] Department of Experimental and Clinical Biomedical Sciences "Mario Serio", University of Florence, Florence, Italy
[c] I.N.B.B. (Istituto Nazionale Biostrutture e Biosistemi), Rome, Italy

ARTICLE INFO

Keywords:
GnRH neurons
Kisspeptin 1 receptor
Hypothalamus-pituitary-gonadal axis
Endocrine disruptors
Polycyclic aromatic hydrocarbon

ABSTRACT

The neuroendocrine control of reproduction is strictly coordinated at the central level by the pulsatile release of gonadotropin-releasing hormone (GnRH) by the hypothalamic GnRH neurons. Alterations of the GnRH-network, especially during development, lead to long-term reproductive and systemic consequences, also causing infertility. Recent evidence shows that benzo[a]pyrene (BaP), a diffuse pollutant that can play a role as an endocrine disruptor, affects gonadal function and gamete maturation, whereas data demonstrating its impact at hypothalamic level are very scarce. This study investigated the effects of BaP (10 μM) in a primary cell culture isolated from the human fetal hypothalamus (hfHypo) and exhibiting a clear GnRH neuron phenotype. BaP significantly decreased gene and protein expression of both GnRH and kisspeptin receptor (KISS1R), the master regulator of GnRH neuron function. Moreover, BaP exposure increased phospho-ERK1/2 signaling, a well-known mechanism associated with KISS1R activation. Interestingly, BaP altered the electrophysiological membrane properties leading to a significant depolarizing effect and it also significantly increased GnRH release, with both effects being not affected by kisspeptin addition. In conclusion, our findings demonstrate that BaP may alter GnRH neuron phenotype and function, mainly interfering with KISS1R signaling and GnRH secretion and therefore with crucial mechanisms implicated in the central neuroendocrine control of reproduction.

1. Introduction

The small neuronal population of gonadotropin-releasing hormone (GnRH)-secreting neurons, located into the preoptic area (POA) of the hypothalamus, represents the central regulator of the hypothalamic-pituitary-gonadal (HPG) axis and controls the initiation and maintenance of reproductive function in mammals. During the human ontogenesis, GnRH-secreting neurons originate outside the brain from progenitors located in the medial part of the olfactory placode and migrate along the route of the olfactory nerves to enter the forebrain and finally reach their appropriate location into the hypothalamus (Casoni et al., 2016; Schwanzel-Fukuda et al., 1996; Wray, 2010). The earliest sign of GnRH-positive cells into the fetal hypothalamus has been detected by the ninth week of gestation (Bloch et al., 1992). Once reached their final location, GnRH neurons conclude their maturation starting to release, in a pulsatile manner, the GnRH peptide into the pituitary portal blood circulation. The latter controls the gonadotropin secretion by the anterior pituitary and, consequently, sex hormone production and gametogenesis at peripheral gonadal level. This activity is effective during gestational and neonatal period, then it is dampened for a long time until specific permissive signals determine the reawakening of GnRH neurons at the onset of puberty, when a complex regulatory network finely regulate the pulsatile GnRH release. In particular, kisspeptin, a peptide encoded by KISS1 gene and produced by a discrete

☆ This paper has been recommended for acceptance by Maria Cristina Fossi.

* Corresponding author. Section of Human Anatomy and Histology, Department of Experimental and Clinical Medicine, University of Florence, L.go Brambilla 3, 50134, Florence, Italy.
E-mail address: a.morelli@unifi.it (A. Morelli).

https://doi.org/10.1016/j.envpol.2022.120766
Received 2 August 2022; Received in revised form 20 October 2022; Accepted 25 November 2022
Available online 29 November 2022

population of hypothalamic neurons, represents the master regulator of GnRH-secreting activity (Tng, 2015) at the puberty onset, as well as during adulthood. Indeed, GnRH neurons express the kisspeptin receptor, KISS1R (also referred to as GPR54), through which the kisspeptin-synthesizing neurons mediate a wide range of hormonal and metabolic signals known to regulate GnRH secretion (Rønnekleiv and Kelly, 2013). Failure of GnRH neuronal migration and/or defects of GnRH system maturation and hormone secretion results in alteration of sex maturation and reproductive competence leading to infertility.

Epidemiological studies and pre-clinical investigations in animal models revealed that increasing environmental pollution is becoming a serious issue for the correct function of the HPG axis and, in general, for human health (Segal and Giudice, 2019). The endocrine-disrupting compounds (EDCs) are ubiquitous contaminants present in the environment in many different forms. They can affect the endocrine homeostasis by altering hormone secretion or their targets and mechanisms of action (Gore et al., 2015; Marraudino et al., 2019; Street et al., 2018). These environmental factors influence the reproductive system by different mechanisms that can be more dangerous during critical periods of development, such as fetal and perinatal life. Benzo[a]pyrene (BaP), a polycyclic aromatic hydrocarbon (PAH), is a harmful and widespread environmental toxicant that acts as EDC (Šimečková et al., 2022). BaP results from the incomplete combustion of organic substances, and it is present in industrial production, forest fires, cigarette smoke, vehicular emissions, contaminated food and water (Alegbeleye et al., 2017). It is also persistent in the environment for long periods due to its limited water solubility and high affinity for particulate matter (Kanaly and Harayama, 2000). Although several studies of chronic BaP exposure demonstrated that cancerogenic risk is the most common outcome, growing evidence indicates that BaP may cause neurodevelopmental and reproductive toxicities in both males and females (Alamo et al., 2019; Bolden et al., 2017). Effects on semen quality and fertility have been reported for men exposed to BaP (Hsu et al., 2006; Soares and Melo, 2008). *In vivo* studies have shown that BaP can cross the blood-testis barrier (Inyang, 2003), causing sperm DNA damage and affecting spermatogenesis (Mohamed et al., 2010; Revel et al., 2001). Moreover, several studies have demonstrated that BaP affects the ovarian follicles and oocyte DNA (Einaudi et al., 2014; Neal et al., 2007; Ramesh et al., 2010). Finally, urine PAH concentration, as a biomarker of BaP exposure, is inversely related to fertilization rate in assisted reproduction (Jeng et al., 2013; Netter et al., 2020).

Despite the extensive research on BaP toxicity at the peripheral gonadal level, very little is known about the effect of BaP exposure at the central level on the GnRH regulatory network. As most lipophilic compounds, BaP can easily cross the blood-brain barrier (BBB), directly reaching neurons in the central nervous system (CNS) (Das et al., 1985; Saunders et al., 2001). Moreover, in the case of GnRH-secreting neurons it is known that they project their dendrites to the circumventricular regions, outside the BBB (Herde et al., 2011), and are therefore particularly vulnerable to circulating toxicants, including BaP. Indeed, the effect of BaP on the CNS has been well documented by several evidences reporting behavioral deficits and cognitive decline both in animal models and in humans (Liu et al., 2020; Niu et al., 2010; Saunders et al., 2006). However, data on central GnRH system alterations by BaP exposure are just limited to few recent researches on teleosts (Gao et al., 2018; Wang et al., 2019). Overall, knowledge about GnRH neurons biology is mainly based on animal models and immortalized cell lines, either of mouse (Mellon et al., 1990; Radovick et al., 1991) or rat (Mansuy et al., 2011) origin, while information from human models are limited. In this regard, we recently demonstrated that BaP exposure interferes with the migratory properties and thereby with the correct maturation of GnRH neuroblasts isolated from the human fetal olfactory epithelium (Guarnieri et al., 2021), while data concerning the effects of BaP on human GnRH neurons at hypothalamic level are still lacking. We previously established and characterized a primary culture of human hypothalamic neurons (hfHypo) with a GnRH-secreting phenotype, isolated from the fetal brain at 12 weeks of gestation (Sarchielli et al., 2017). This stage of fetal development corresponds to a wide distribution of GnRH cell bodies and fibers in the hypothalamus (Casoni et al., 2016). In the present study, we took advantage of hfHypo cells to better identify the effects of BaP exposure on human GnRH neuron maturation and function. Although obtained *in vitro* in a simple model, the results are the first evidence of the deleterious effects of BaP in GnRH neurons of human origin.

2. Materials and methods

2.1. Cell cultures and reagents

All the experiments were performed using a primary culture of human fetal GnRH-secreting neurons (hfHypo) previously established and characterized (Sarchielli et al., 2017). The cell culture was isolated from the hypothalamus of a 12-week old fetus from voluntary abortions according to the Italian National Institute of Health ethical guidelines, after written informed consent of the mother (ID: 20,028/13, released on 09/20/2013) and with the approval of National Ethics Committee and the local Ethics Committee for investigation in Humans (Protocol Number: 678,304; University of Florence). Briefly, tissue was enzymatically digested and dispersed by pipetting in an appropriate culture medium (Coon's modified Ham's F12; Sigma-Aldrich Corp., St. Louis, MO, USA) with the supplementation of 10% fetal bovine serum (FBS; Euroclone, Milan, Italy). hfHypo cells were cultured in a controlled atmosphere (5% CO_2) at the temperature of 37 °C. BaP (Sigma-Aldrich Corp.) was dissolved in dimethylsulfoxide (DMSO; Sigma-Aldrich Corp.) at 50 mM concentration as stock solution.

2.2. Immunocytochemistry

GnRH immunostaining was performed as already reported (Guarnieri et al., 2021). Briefly, hfHypo cells were fixed using paraformaldehyde 2% dissolved in PBS (phosphate buffered saline; Sigma-Aldrich Corp.), permeabilized with Triton X-100 0.1% (Sigma-Aldrich Corp.) and blocked with BSA 1% (bovine serum albumin; Sigma-Aldrich Corp.). Immunofluorescence staining was performed using a rabbit polyclonal anti-GnRH primary antibody (1:100; Abcam, Cambridge, UK), followed by incubation with Alexa Fluor 488-conjugated secondary antibodies (1:200; Molecular Probes, Eugene, OR, USA). ProLong Gold antifade reagent with 4′,6′-diamidino-2-phenylindole dihydrochloride (DAPI; Molecular Probes) was used for mounting slides and counterstaining nuclei. Images were collected using Nikon Microphot-FXA microscope (Nikon, Tokyo, Japan).

2.3. Flow cytometry

Flow cytometry analysis was performed as previously published (Guarnieri et al., 2021). Briefly, hfHypo cells (2×10^5) were firstly fixed in PBS with paraformaldehyde 2%, next resuspended in wash buffer (PBS with 1% FBS), incubated with anti-GnRH (1:100; Abcam) and anti-KISS1R (1:150; Alomone Labs, Jerusalem, Israel) primary antibodies, followed by the staining with the secondary antibody Alexa Fluor 488 goat anti-rabbit IgG (1:200; Molecular Probes). Negative controls were assessed by avoiding anti-GnRH and anti-KISS1R primary antibodies, while autofluorescence was evaluated in cells without both primary and secondary antibodies. Cells preparations were evaluated on a FACSCanto II instrument (BD Pharmingen). BD FACSDiva Software (BD) and FlowJo v10 (Tree Star Inc., Ashland, OR, USA) were used to analyze the obtained data. At least three separate experiments were assessed for obtaining statistical significance (Whittaker et al., 2015).

2.4. Quantitative RT-PCR analysis

Gene expression analysis was performed by quantitative real-time RT-PCR (qRT-PCR) as previously published (Sarchielli et al., 2017), with minor modifications. First, RNeasy Mini kit (Qiagen, Hilden, Germany) and iScript™ cDNA Synthesis Kit (Bio-Rad Laboratories, Hercules, CA, USA) were used for RNA extraction from 2×10^5 hfHypo cells and cDNA synthesis, respectively, both following the manufacturers' instructions. Quantitative expression of target genes by qRT-PCR was performed using SsoAdvanced Universal SYBR® Supermix and the CFX96 Two-Color Real-Time PCR Detection System (both Bio-Rad Laboratories), as appropriate. Specific primers and probes used were predeveloped assays by Life Technologies (Carlsbad, CA, USA) or custom made by sequences available at NCBI GenBank (https://www.ncbi.nlm. nih. gov/) or Ensemble Genome (http://www.ensembl.org). The 18 S ribosomal RNA subunit was measured with a predeveloped assay (Hs99999901_s1, Life Technologies) and taken as reference gene for the quantitation of the target genes. Relative quantification was performed using the comparative threshold cycle (Ct) $2^{-\Delta\Delta Ct}$ method (Livak and Schmittgen, 2001). At least three separate experiments, each including three independent biological replicates, were performed and analyzed for obtaining statistical significance.

2.5. MTT assay

BaP cytotoxicity was assessed by MTT assay (Sigma-Aldrich Corp.) as already described (Guarnieri et al., 2020). hfHypo cells (8×10^3 per well) were seeded in 96 multi-well plates and, after 24 h, serum-starved (8 h) and then treated with different concentrations of BaP (0.2, 1, 10, 20 and 60 μM) for additional 24 h. Culture medium was next discarded and equal amount of MTT solution (Sigma-Aldrich Corp.) was added for 3 h at 37 °C. The absorbance was read at 450 nm using a Multiscan FC spectrophotometer (Thermo Fisher Scientific, Waltham, MA, USA). Data were shown as a percentage of the control, taken as 100% (mean ± SEM). All experiments were in quadruplicate and at least three different experimental setups were assessed for obtaining statistical significance.

2.6. Intracellular ROS detection

Intracellular ROS production was analyzed by flow cytometry using the oxidation-sensitive fluorescent probe H2DCF-DA (Invitrogen, Carlsbad, CA, USA), as already described with minor modifications (Pensalfini et al., 2008). Briefly, 2×10^5 hfHypo cells were washed in PBS and incubated with 1 μM H2DCF-DA in pre-warmed DMEM medium without serum and phenol red for 30 min at 37 °C in the dark. H2DCF-DA is a non-fluorescent indicator that can easily penetrate the cells where can be oxidized by ROS generating the fluorescent form 2′, 7′-dichlorofluorescein (DCF). After labeling, hfHypo cells were washed and resuspended in PBS and immediately analyzed using a FACSCanto™ flow cytometer (Becton-Dickinson, San Jose, CA, USA). The cell flow rate was set to about 1000 cells/s and the gates were defined by forward- and side-scatter measurements of the relative unlabelled cell population. Negative controls were assessed analyzing autofluorescence of unstained cells. The fluorescence properties of 20,000 cells were collected and analyzed using FloJo software (Tree Star, Inc.) (Becatti et al., 2016). Three different sets of experiments were assessed for obtaining statistical significance.

2.7. Total antioxidant capacity (TAC) assay

Total antioxidant capacity (TAC) was estimated by oxygen radical absorbance capacity (ORAC) method as previously described, with minor modifications (Becatti et al., 2018). Briefly, 6 nM fluorescein solution (from a 4 μM stock) was prepared in 75 mM sodium phosphate buffer with pH 7.4, at the time of the experiment. Trolox, a water-soluble vitamin E analog, was used as standard-solution at final concentration of 250 μM. Protein lysate of each sample was pre-incubated with 100 μL of fluorescein solution for 30 min at 37 °C, before rapidly adding 19 mM 2, 2′-azobis (2-amidinopropane) dihydrochloride (AAPH) solution. Fluorescence emitted by the oxidation of fluorescein after the thermal decomposition of AAPH was detected by a Fluoroskan Ascent Microplate Fluorometer (Thermo Fisher Scientific) with 485 nm excitation and 537 nm emission. Data were reported as Trolox Equivalents (μM) normalized for protein concentration. Three different experiments were assessed for obtaining statistical significance.

2.8. GnRH release assay

The GnRH release in the culture medium was measured using LH-RH Fluorescent EIA Kit (Phoenix Pharmaceuticals Inc., Burlingame, CA, USA) according to manufacturer's instructions. Briefly, 2×10^5 hfHypo cells were cultured in serum-free condition in the presence or absence of BaP (10 μM) for 24 h. Collected media were purified using Strata C18/E 200 mg/3 ml columns (Phenomenex, Torrance, CA, USA) and lyophilized with LIO-5P DIGIT instrument (Tecnodinamica Moderna srl, Monterotondo Scalo, Italy), as previously described (Morelli et al., 2008). Next, lyophilized samples were reconstituted in 150 μl of assay buffer and immediately used for the GnRH quantification. The resulting fluorescence was evaluated with BioTek Synergy H1 Hybrid plate reader (Agilent, Santa Clara, CA, USA). Three separate experiments, each including three independent biological replicates, were performed and analyzed for obtaining statistical significance.

2.9. Western blotting

Extraction of protein from 2×10^5 hfHypo cells was performed using the RIPA buffer (Thermo Fisher Scientific) with the addition of protease inhibitors cocktails (1:100; Sigma-Aldrich Corp.) according to the manufacturers' instruction. Quantification of the protein extracts was carried out by Coomassie protein assay kit (Bio-Rad Laboratories). Aliquots containing 30 μg of protein extract were processed for immunoblotting as previously reported (Sarchielli et al., 2018). Briefly, proteins extracts were subjected to protein molecular weight on SDS-PAGE and transferred on polyvinylidene difluoride membranes (GE Healthcare, Little Chalfont, UK). After blocking in 3% BSA in PBS, membranes were incubated with the following primary antibodies: mouse monoclonal anti-pERK1/2 (Cell Signaling Technology, Danvers, MA, USA; 1:2000), rabbit polyclonal anti-ERK1/2 (Cell Signaling Technology; 1:1000), rabbit polyclonal anti-KISS1R (Alomone Labs; 1:500), and rabbit polyclonal anti-α-tubulin (Cell Signaling Technology; 1:1000). Peroxidase-conjugated secondary anti -mouse or -rabbit antibodies (Santa Cruz Biotechnology, CA, USA) were used (1:5000 in PBS), as appropriate. Blots were visualized using the enhanced chemiluminescence system LiteAblot extend (Euroclone) and the acquisition was achieved with Amersham Hyperfilm (GE Healthcare). Densitometric analysis was quantified by ImageJ software (https://imagej.net/) and α-tubulin protein was used as reference for normalization. At least four different experiments were assessed for obtaining statistical significance.

2.10. Electrophysiological records

The whole cell patch-clamp technique, both in current- and voltage-clamp conditions, was performed as previously described (Sarchielli et al., 2017). The cells were continuously superfused with a physiological solution having the following composition (mM): 150 NaCl, 5 KCl, 2.5 $CaCl_2$, 1 $MgCl_2$, 10 D-glucose and 10 HEPES. The patch pipettes were filled with an internal solution containing (mM): KCl 130, NaH_2PO_4 10, $CaCl_2$ 0.2, EGTA 1, MgATP 5 and HEPES/KOH 10. Once filled, the pipette resistance measured 1–2 MΩ. The pH was set to 7.4 with NaOH for external solution and to 7.2 with tetraethyl ammonium hydroxide (TEA-OH) for the internal solution.

The resting membrane potential (RMP) was recorded in the current-clamp mode, by applying a stimulus I = 0 nA. The membrane passive properties, cell resistance (R_m), resting conductance (G_m) and linear capacitance (C_m), were evaluated in voltage clamp mode starting from a holding potential (HP) of −70 mV, by applying two 75-ms step voltage pulses to −80 and −60 mV, as detailed in previous papers (Squecco et al., 2015). The R_m and its reciprocal value, G_m (calculated from $1/R_m$), are indicative of the membrane permeability, whereas C_m is related to the cell surface area. Thus, the ratio G_m/C_m represents the specific conductance.

The currents flowing through transient receptor potential canonical (TRPC)-like cationic channels were isolated with the use of $GdCl_3$, as previously published (Sarchielli et al., 2017). Briefly, we applied a pulse protocol of stimulation consisting of 200-ms step pulses ranging from −80 to 0 mV, in 10 mV-increments, starting from a HP = −60 mV. The current actually flowing through TRPC (I_{TRPC}) was obtained by subtracting from the current evoked by the test pulses the residual current recorded at least 3 min after the addition of the TRPC blocker gadolinium chloride ($GdCl_3$; 50 μM; Sigma-Aldrich Corp.) in the bath solution at the end of the trial.

To compare correctly the currents recorded from different cells, the current amplitude was consistently normalized to C_m, and reported as current density, I/C_m.

2.11. Statistical analysis

Data were expressed as mean ± standard error of mean (SEM), or standard deviation (SD) or median ± interquartile range, as appropriate. Student's unpaired *t*-test or one-way ANOVA followed by Bonferroni's correction for multiple comparison were performed, as appropriate, to determine statistical significance which was defined as $p < 0.05$. In the electrophysiological experiments n represents the number of cells. Results were evaluated using the Statistical Package for the Social Sciences (SPSS v.28.0; SPSS Inc., Chicago, IL, USA; https://www.ibm.com/support/pages/downloading-ibm-spss-statistics-25).

3. Results

3.1. Cytotoxicity and metabolism of BaP in hfHypo

The GnRH phenotype of hfHypo cells was confirmed as already published (Sarchielli et al., 2017). In particular, the identity of hfHypo as GnRH-secreting neurons was demonstrated by a strong immunopositivity to GnRH, as assessed by both immunocytochemistry and flow cytometry analyses (Fig. 1A and B). By qRT-PCR analysis, we also confirmed that hfHypo cells express specific genes of the GnRH neuron phenotype, such as the neuronal marker β-tubulin III as well as GnRH1 and KISS1R (Fig. 1C). Moreover, to better characterize the hfHypo cells phenotype, we analyzed the expression of sex hormone receptors

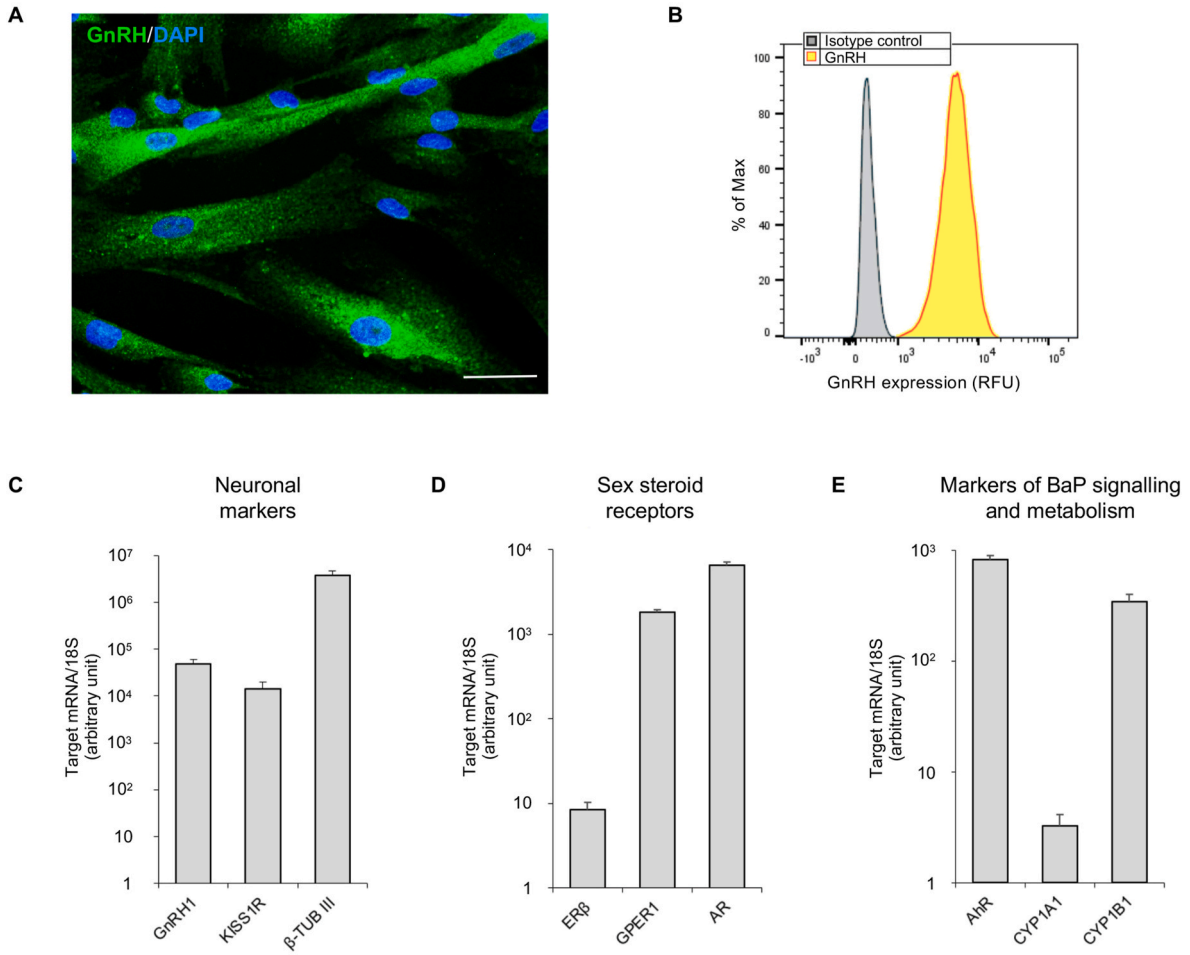

Fig. 1. Hypothalamic GnRH neurons characterization and mRNA expression profile of hfHypo culture. A) Representative image of hfHypo cells expressing GnRH (green) as demonstrated by immunofluorescence analysis; blue-colored DAPI counterstained nuclei are also shown; scale bar: 50 μm. B) Representative overlaid histogram of GnRH expression (yellow peak), as detected in hfHypo cells by flow cytometry analysis. Negative control is light grey peak. (C–E) Relative mRNA expression by qRT-PCR analysis of target genes normalized over 18 S ribosomal RNA subunit, taken as the housekeeping gene, and showed as mean ± SEM (n = 9). (For interpretation of the references to color in this figure legend, the reader is referred to the Web version of this article.)

implicated in GnRH neuron function and we observed high mRNA levels of the androgen receptor (AR) and the membrane estrogen receptor GPER1 (G Protein-Coupled Estrogen Receptor 1) accompanied by low expression levels of the nuclear ERβ transcripts, while ERα mRNA expression was not detected (Fig. 1D). In addition, to explore the ability of hfHypo cells to directly respond and metabolize BaP, we verified that hfHypo cells expressed high levels of aryl hydrocarbon receptor (AhR) mRNA, which mediates intracellular signaling of BaP, as well as both CYP1A1 and CYP1B1, two cytochrome P450 isoforms responsible for the metabolic activation of BaP, with CYP1B1 mRNA being more abundant than CYP1A1 (Fig. 1E).

We next evaluated the cytotoxicity of BaP on hfHypo cells by MTT assay. After 24 h of treatment, BaP (0.2–60 μM) induced significant cytotoxicity in cells at concentrations greater than 10 μM, as compared to untreated cells ($p < 0.001$; Fig. 2A). Based on these results the sub-toxic concentration of 10 μM BaP was used for the subsequent experiments, as relevant and commonly chosen concentration for *in vitro* toxicity studies (Sarma et al., 2017; Slotkin and Seidler, 2009; Zhang et al., 2022) and also selected as environmentally relevant dose (Chen et al., 2012; Slotkin et al., 2013).

Exposing hfHypo to BaP (10 μM for 24 h) induced a significant decrease of AhR mRNA ($p < 0.05$; Fig. 2B), while both CYP1A1 and CYP1B1 mRNA levels were significantly increased ($p < 0.001$; Fig. 2C and D, respectively), as expected by the BaP-induced mechanisms for these isoforms (Gelboin, 1980). In addition, a significant increase in gene expression of cyclooxygenase-2 (COX-2), an inducible enzyme associated to inflammation, was also observed in hfHypo cells treated with BaP (10 μM for 24 h; $p < 0.001$; Fig. 2E), while mRNA expression of the proinflammatory cytokine TNFα was unchanged by BaP exposure (10 μM for 24 h; Fig. 2F).

Based on previous studies demonstrating that BaP and its metabolites produce reactive oxygen species (ROS), which may cause oxidative stress (Ji et al., 2013), we analyzed ROS generation in hfHypo cells. As detected by the flow cytometry analysis, using a specific indicator of cellular oxidative stress (H2DCF-DA), treating hfHypo with BaP (10 μM for 24 h) significantly increased ROS production in comparison with control cells ($p < 0.05$; Fig. 2G). We also observed that BaP determined a significant 30% increase in total antioxidant capacity (TAC) in hfHypo

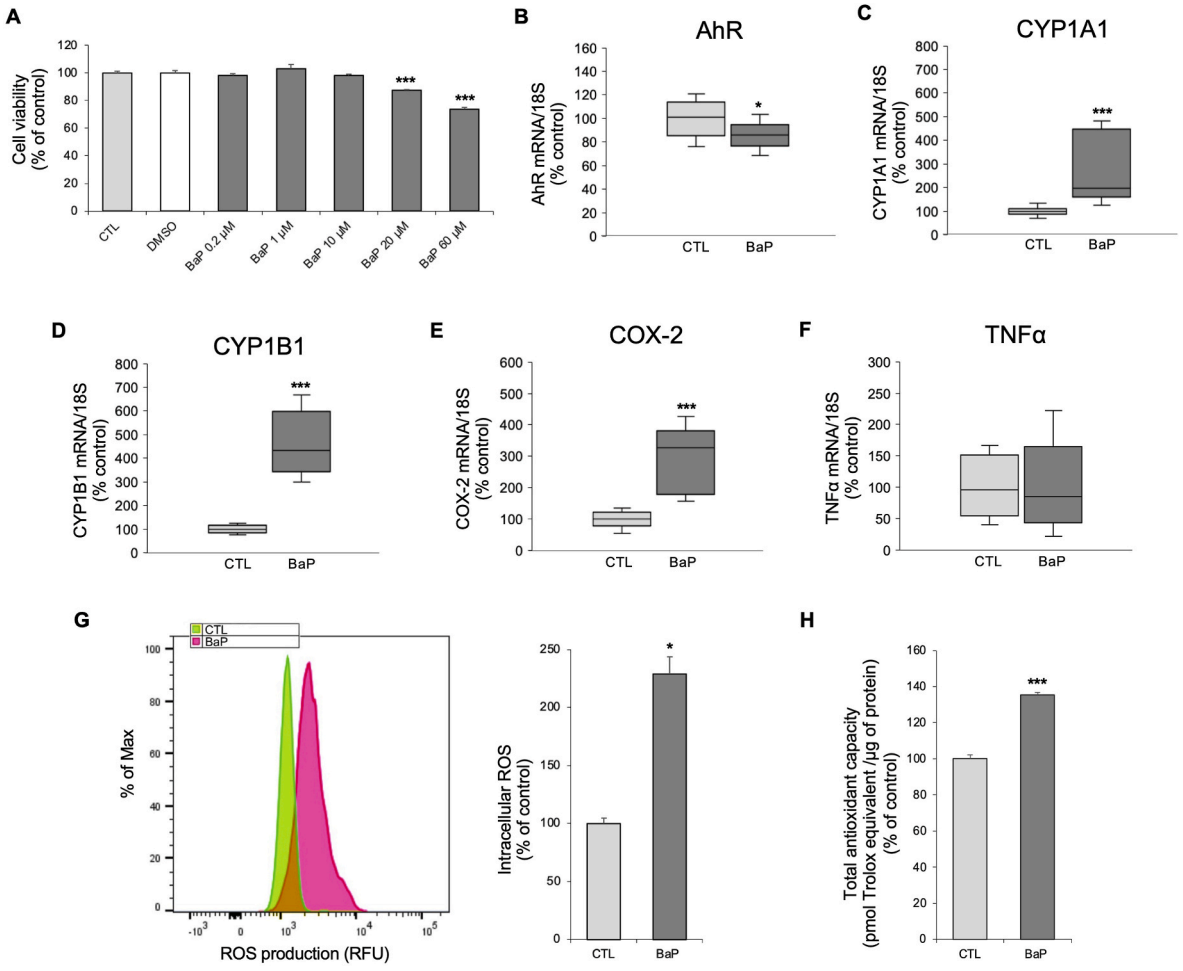

Fig. 2. Cytotoxicity and effects on target genes of BaP in hfHypo cells. A) MTT analysis of BaP-treated hfHypo cells at different concentrations (0.2, 1, 10, 20 and 60 μM) for 24 h (dark grey bars); vehicle control (DMSO; white bar) was also included in the analysis; cell viability was reported as percentage of viable cells over control (untreated cells; CTL; light grey bar), taken as 100% (mean ± SEM; n = 12). B–F) qRT-PCR analysis indicating mRNA expression of target genes (AhR, arylic hydrocarbon receptor; CYP1A1, cytochrome P450 1A1 isoform enzyme; CYP1B1, P450 1B1 isoform enzyme; COX-2, cycloxygenase-2, TNFα, tumor necrosis factor α) in untreated (CTL, light grey box) and BaP-treated (10 μM for 24 h; dark grey box) hfHypo cells. Data are normalized over 18 S ribosomal RNA subunit, taken as the housekeeping gene, expressed as percentage of CTL (median ± interquartile range; n = 9). G) Representative overlaid histogram (left) and the bar graph (right) of intracellular reactive oxygen species (ROS) production in hfHypo cells with (BaP, pink peak, dark grey bar) or without (CTL, green peak, light grey bar) BaP exposure (10 μM 24 h), as detected by flow cytometry analysis. Data are expressed as percentage of CTL (mean ± SEM; n = 3). H) Total antioxidant capacity in untreated (CTL, light grey box) and BaP-treated (10 μM 24 h; dark grey box) hfHypo cells. Data are expressed as Trolox Equivalents (pmol), normalized for protein concentration (μg) and reported as percentage of CTL (mean ± SEM; n = 3). Statistical analysis was performed using unpaired Student's t-test; *$p < 0.05$, ***$p < 0.001$ vs. CTL. (For interpretation of the references to color in this figure legend, the reader is referred to the Web version of this article.)

cells, as detected by ORAC chemiluminescence method ($p < 0.05$; Fig. 2H), thus confirming the presence of oxidative insult.

3.2. BaP affects GnRH neuron function

We next verified if BaP might interfere with GnRH neuron phenotype and function. Gene expression analysis by qRT-PCR demonstrated that 24 h exposure to BaP (10 μM) significantly reduced GnRH1 mRNA levels, when compared to untreated cells ($p < 0.001$; Fig. 3A), with no effects on β-tubulin III mRNA expression (data not shown). Moreover, as compared to untreated cells, BaP exposure significantly reduced AR ($p < 0.05$; Fig. 3B) and increased GPER1 ($p < 0.01$; Fig. 3C), without changing ERβ mRNA expression (data not shown). Flow cytometry analysis demonstrated that BaP (10 μM for 24 h) significantly decreased GnRH levels in hfHypo cells also in terms of protein expression ($p < 0.01$; Fig. 3D). In particular, BaP significantly reduced the percentage of GnRH-positive cells (46.93 ± 4.66%) when compared to untreated cells (78.47 ± 3.38%; $p < 0.01$; Fig. 3E). Interestingly, when we analyzed the GnRH-secreting ability of hfHypo cells we found that the amount of GnRH released by the cells in the culture medium was significantly increased by BaP exposure (10 μM for 24 h), as compared to untreated cells ($p < 0.01$; Fig. 3F).

To further characterize the effect of BaP, we analyzed if the pollutant might alter the response of hfHypo cells to kisspeptin. As shown in Fig. 4 (panels A–C), BaP exposure (10 μM for 24 h) significantly reduced both gene ($p < 0.05$) and protein ($p < 0.01$) expression of KISS1R in comparison to untreated cells. Moreover, as expected (Kotani et al., 2001; Sarchielli et al., 2017), exposing hfHypo cells to kisspeptin (1 μM for 15 min) determined a phospho-ERK1/2 increase, as evaluated by Western blot analysis ($p < 0.01$; Fig. 4D). Interestingly, BaP treatment (10 μM) for 24 h determined a significant induction of phospho-ERK1/2 and the addition of kisspeptin (1 μM for 15 min; $p < 0.01$) in BaP-treated cells did not further increase this expression (Fig. 4D).

3.3. BaP affects electrophysiological properties and kisspeptin-mediated response of hfHypo

Since hfHypo cells depolarize and release GnRH peptide in response to kisspeptin by the activation of transient receptor potential canonical (TRPC) channels (Zhang et al., 2008), we next performed electrophysiological experiments to verify this functional aspect. As already reported (Sarchielli et al., 2017), we confirmed that hfHypo cells normally exhibited a resting membrane potential (RMP) of −45.8 ± 7.4 mV, which resulted significantly depolarized after the addition of kisspeptin (1 μM) to the bath solution ($p < 0.01$; Fig. 5A). In the presence of $GdCl_3$ (50 μM), the specific blocker of TRPC channels, kisspeptin was no more able to depolarize the cells (Fig. 5A). Pretreating hfHypo cells with BaP (10 μM for 24 h) caused a significant depolarization of the RMP compared to control cells that was not affected by the addition of kisspeptin, nor by $GdCl_3$ ($p < 0.01$; Fig. 5A). However, BaP (10 μM for 24 h) caused a significant decrease of cell resistance values, R_m, compared to untreated cells ($p < 0.05$; Fig. 5B), suggesting the ability of the pollutant to determine some ion channels and/or hydrophilic pores to open, most likely independently from TRPC activation.

To further investigate the mechanism through which BaP altered cell membrane potential and better clarify if the unresponsiveness to kisspeptin of BaP-treated cells was due or not to interference with TRPC channels, we analyzed other electrophysiological parameters, such as the specific conductance, G_m/C_m (Fig. 5C). While the patch clamp recordings in control hfHypo cells showed that kisspeptin (1 μM) induced a significant 3-fold increase of G_m/C_m ($p < 0.01$), which was markedly inhibited by $GdCl_3$ (50 μM), the pretreatment with BaP (10 μM for 24 h)

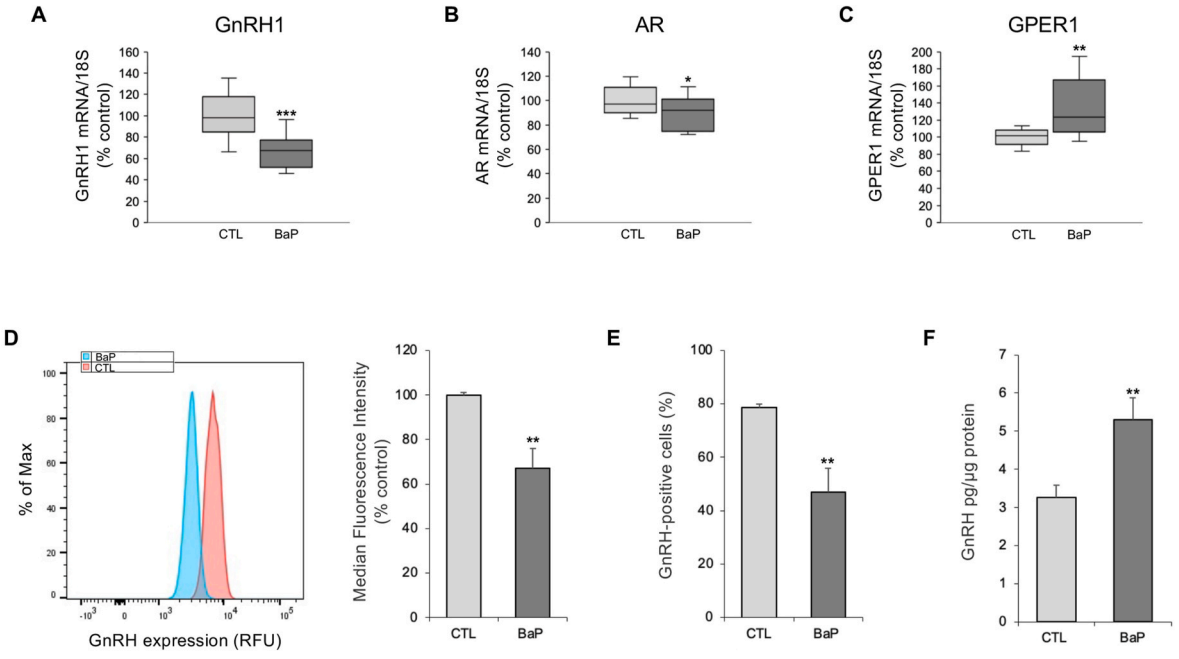

Fig. 3. Effect of BaP on GnRH neurons phenotype. A-C) qRT-PCR analysis showing mRNA expression of target genes (GnRH1, gonadotropin-realizing hormone; AR, androgen receptor; GPER1, G Protein-Coupled Estrogen Receptor 1) in untreated (CTL, light grey box) and BaP-treated (10 μM 24 h; dark grey box) hfHypo cells. Data are normalized over 18 S ribosomal RNA subunit, taken as the housekeeping gene, and expressed as percentage of CTL (median ± interquatile range; n = 9). D) Representative overlaid histogram (left) and the bar graph (right) showing the mean fluorescence intensity for GnRH protein in control (untreated cells, CTL, red peak, light grey bar), taken as 100%, and BaP-treated (10 μM for 24 h, light blue peak, dark grey bar), as detected in hfHypo cells by flow cytometry analysis. Data are reported as mean ± SEM (n = 3). E) Bar graph showing the percentage of GnRH-positive cells in untreated (CTL, light grey bar) and BaP-treated (10 μM for 24 h, dark grey bar) hfHypo cells, as detected by flow cytometry analysis. Data are reported as percentage of positive cells (mean ± SEM; n = 3). F) GnRH secretion in the culture medium by hfHypo cells treated or not (CTL) with BaP (10 μM 24 h), as detected by fluorescent immunoassay. Results are expressed as GnRH concentration (pg) per μg of protein and reported as mean ± SEM (n = 9). Statistical analysis was performed using unpaired Student's t-test; *$p < 0.05$, **$p < 0.01$, ***$p < 0.001$ vs. CTL. (For interpretation of the references to color in this figure legend, the reader is referred to the Web version of this article.)

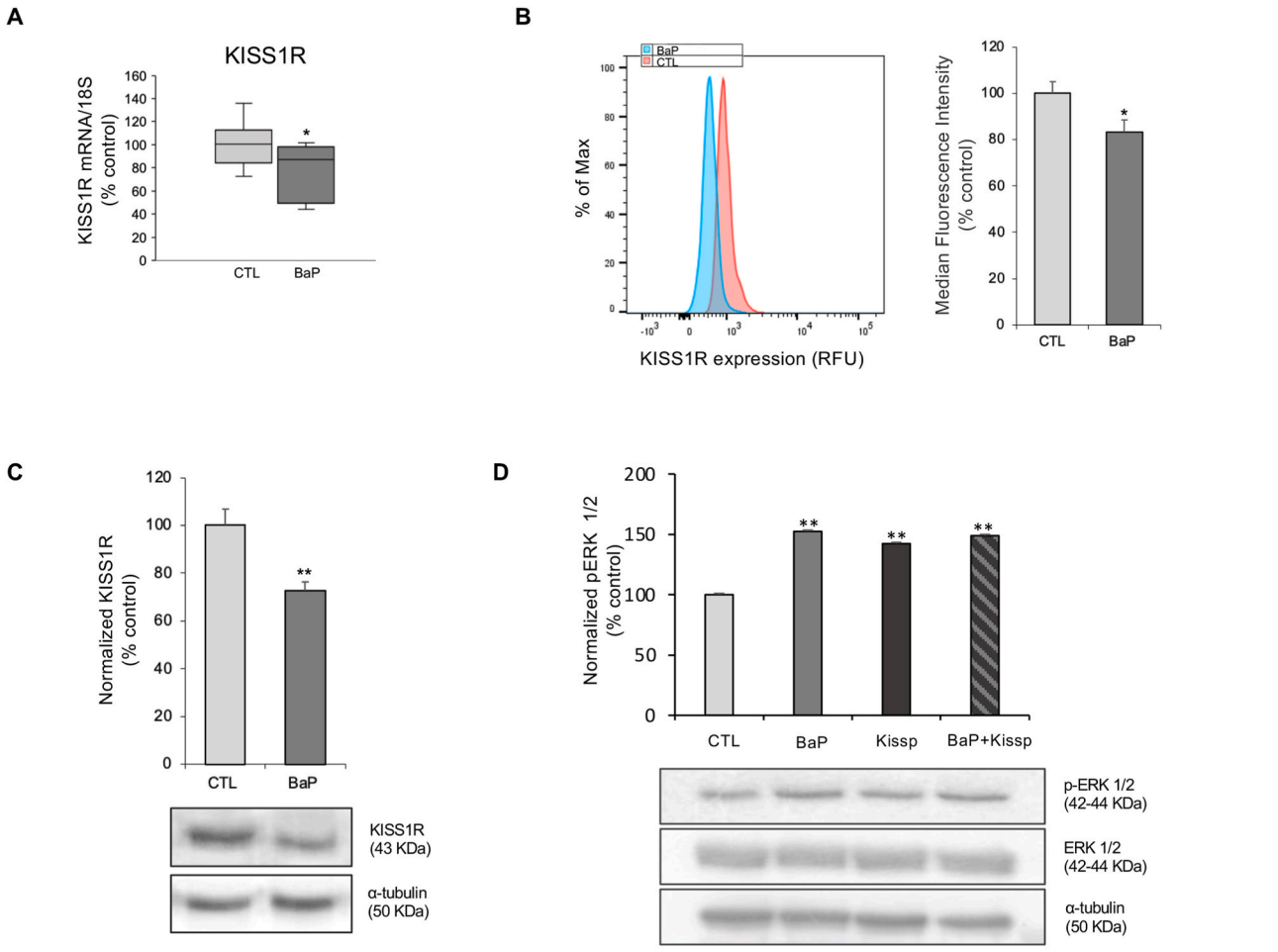

Fig. 4. Effect of BaP on KISS1R-mediated signaling in hfHypo cells. A) mRNA expression of KISS1R in untreated (CTL, light grey box) and BaP-treated (10 μM 24 h; dark grey box) hfHypo cells. Data are normalized over 18 S ribosomal RNA subunit, taken as the housekeeping gene, expressed as percentage of CTL (median ± interquatile range; n = 9). B) Representative overlaid histogram (left) and the bar graph (right) showing the mean fluorescence intensity for KISS1R protein in control (untreated cells, CTL, red peak, light grey bar), taken as 100%, and BaP-treated (10 μM for 24 h, light blue peak, dark grey bar), as detected in hfHypo cells by flow cytometric analysis. Data are reported as mean ± SEM (n = 4). C) Western blot analysis of KISS1R in untreated (CTL, light grey bar) and BaP-treated (10 μM 24 h, dark grey bar) hfHypo cells. α-tubulin immunodetection were used for normalization. Data are expressed as percentage of CTL, taken as 100%, and reported as mean ± SEM (n = 6). D) Western blot analysis of ERK 1/2 phosphorylation in untreated (CTL), BaP- (10 μM) and/or kisspeptin-treated (1 μM) hfHypo cells for 24 h. ERK1/2 and α-tubulin immunodetection were used for normalization. Data are expressed as percentage of CTL, taken as 100%, and reported as mean ± SEM (n = 4). Statistical analysis was performed using unpaired Student's t-test, *$p < 0.05$, **$p < 0.01$ vs. CTL. (For interpretation of the references to color in this figure legend, the reader is referred to the Web version of this article.)

did not affect G_m/C_m measures compared to control cells. Kisspeptin (1 μM) addition to the bath solution in BaP-treated cells again did not induce significant increase of G_m/C_m, and likewise adding $GdCl_3$ (50 μM) in this condition did not cause further changes (Fig. 5C).

We next analyzed the currents evoked by a voltage step pulse protocol. Consistent with previous observations (Sarchielli et al., 2017) acute addition of kisspeptin (1 μM) to the bath solution induced a clear increase of current amplitude, that reverted towards control values in the presence of $GdCl_3$ (Fig. 5D). Notably, the baseline current (indicated by the red arrow in Fig. 5D), positively related to the ion fluxes through TRPC channels (Formigli et al., 2009), showed different values in the three conditions, being increased by kisspeptin, and decreased towards control values by $GdCl_3$ addition (50 μM), as compared to control. In contrast, the current traces evoked from BaP-treated cells showed a similar baseline current in the three conditions (Fig. 5D), suggesting a scarce effect of kisspeptin on TRPC current in cells pretreated with BaP. In addition, when compared to records obtained in control hfHypo cells, BaP-treated cells exhibited a quite different time course of the test currents evoked by voltage steps that were more positive than −30/-20 mV, almost lacking the early outward transient current.

The kisspeptin-sensitive current flowing through TRPC was estimated by the point-by-point subtraction of the current traces recorded after $GdCl_3$ addition from the total current traces evoked by kisspeptin (Fig. 5D). The evaluation of the amount of TRPC current measured at the end of the test pulses (response region of the pulse protocol) as a function of the voltage test applied showed that kisspeptin-sensitive currents flowing through TRPC (I_{TRPC}) were significantly reduced in BaP-treated hfHypo cells compared to those recorded in untreated cells ($p < 0.05$; Fig. 5E).

4. Discussion

The correct control of puberty onset and the maintaining of reproductive function is guaranteed by a sophisticate neuroendocrine network that crucially depends on the regulation of pulsatile GnRH release by hypothalamic neurons. Environmental perturbations, especially during fetal and pubertal development, were demonstrated to compromise the normal reproductive maturation (Lopez-Rodriguez et al., 2020). In this report, we describe for the first time that the function of human GnRH-secreting neurons is altered by the exposure to

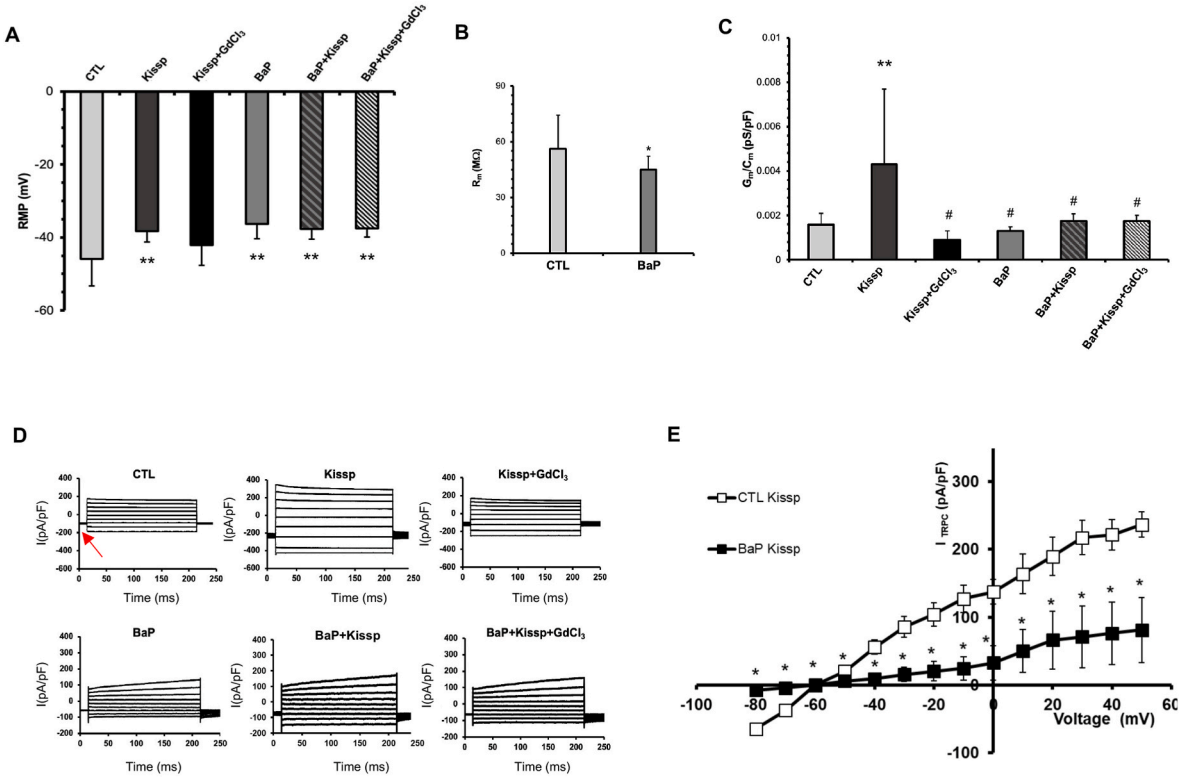

Fig. 5. Effect of BaP on membrane electrophysiological property and kisspeptin responsiveness in hfHypo cells. A) Effect of kisspeptin (Kissp) on RMP (mV) in untreated (CTL) and BaP-treated (10 μM 24 h) hfHypo cells in the absence or presence of TRPC blocker $GdCl_3$. Data are reported as mean ± SD of n analyzed cells. Statistical analysis was performed using One way ANOVA, Bonferroni's post hoc test, **$p < 0.01$ vs CTL (CTL, n = 12; Kissp, n = 10; Kissp + $GdCl_3$, n = 11; BaP, n = 10; BaP + Kissp, n = 10; BaP + Kissp + $GdCl_3$, n = 10). B) R_m (MΩ) values recorded from untreated (CTL; light grey bar) and BaP-treated (10 μM 24 h; dark grey bar) hfHypo cells. Data are reported as mean ± SD of n analyzed cells. Statistical analysis was performed using unpaired Student's t-test, *$p < 0.05$ vs. CTL (CTL, n = 17; BaP, n = 6). C) G_m/C_m (pS/pF) values analysis in untreated cells (CTL) showing a marked increase due to kisspeptin (Kissp) and a following inhibition due to $GdCl_3$ only in CTL cells and not in BaP-treated cells. Data are reported as mean ± SD of n analyzed cells. Statistical analysis was performed using One way ANOVA, Bonferroni's post hoc test, **$p < 0.01$ vs CTL; #$p < 0,05$ vs Kissp. (CTL, n = 7; Kissp, n = 6; Kissp + $GdCl_3$, n = 6; BaP, n = 6; BaP + Kissp, n = 5; BaP + Kissp + $GdCl_3$, n = 5). D) Representative families of current traces evoked from an untreated hfHypo cell (CTL; upper row) or in a BaP-treated cell (10 μM 24 h; lower row) without any substance added (left panels), in the presence of 1 μM kisspeptin (Kissp; middle panels) and in the presence of Kissp + $GdCl_3$ (right panels). The baseline current is indicated by the red arrow. E) Mean values of the kisspeptin-sensitive TRPC current (pA/pF) evoked in untreated (CTL) and BaP-treated (10 μM 24 h) hfHypo cells reported as a function of the voltage step applied. The current values, normalized to cell capacitance C_m, are obtained from the point-by-point subtraction of currents evoked by the voltage step protocol of stimulation recorded after kisspeptin (Kissp) addition, in the absence or presence of 50 μM $GdCl_3$. Data are mean ± SD of n analyzed cells. Error bar is visible when its size exceeds the symbol dimension. Statistical analysis was performed using unpaired Student's t-test, *$p < 0.05$. (CTL, n = 4; BaP, n = 4).

the environmental pollutant BaP, which has already been implicated as EDC in affecting the peripheral gonadal function and consequent fertility both in males and females (Bukowska et al., 2022). As we recently demonstrated (Guarnieri et al., 2021), BaP exposure affects the migratory properties of GnRH-secreting neuron precursors isolated from the human fetal olfactory epithelium (fetal neuroblast cells B4, FNCB4), thus interfering with a critical function of these cells that need to migrate towards the hypothalamus in order to complete their maturation. The results obtained in the present study using the hfHypo cells strongly suggest that also GnRH-secreting neurons within the hypothalamus may represent a target for BaP-induced toxicity, thereby leading to HPG axis alterations. Indeed, hfHypo cells possess all features indicative of GnRH-secreting neuron phenotype (expression of specific markers, including β-tubulin III, GnRH and KISS1R) and function (responsiveness to kisspeptin, activating specific currents and release of GnRH peptide in the culture medium) (Sarchielli et al., 2017). All these features were affected by BaP exposure, demonstrating the ability of these neurons to metabolize the pollutant. Accordingly, hfHypo cells express the nuclear receptor AhR, a well-known mediator of BaP toxicity (Pieterse et al., 2013) as well as the AhR target genes CYP1A1 and CYP1B1, which encode for the main cytochrome P450 enzymes implicated in the bioactivation of BaP (Uppstad et al., 2010).

The strong induction after BaP exposure of both enzyme isoforms demonstrates that GnRH-secreting neurons may be a direct target of BaP, which could act not only at peripheral level on gonadal function, but also at the brain level. Remarkably, BaP exposure determined a significant decrease of AhR mRNA expression in hfHypo cells, thus definitely confirming the activation of AhR-mediated signaling, which, in fact, is known to be downregulated by a negative feedback mechanism, due to the CYP1A1 activity (Schiering et al., 2017).

Several evidences indicate that BaP is a potent pro-oxidative agent in both human and animal models (Adedara et al., 2015; Chiba et al., 2011; Sun et al., 2021). Our data confirm that BaP generates ROS in the brain, as already reported (Adedara et al., 2015; Saha et al., 2020). A significant increase in ROS production was found in BaP-treated hfHypo cells and, interestingly, this activity was accompanied by a significant increase in the total antioxidant capacity of hfHypo cells, suggesting a possible early compensatory mechanism aimed at restoring homeostatic balance (Moreira et al., 2006). Our results are consistent with previous reports of activation of antioxidant mechanisms following BaP stimulation in human trophoblasts (Dong et al., 2016) and in human T-lymphoblasts (Nguyen et al., 2010).

With regard to the effect of BaP on the GnRH neuron phenotype we observed a significant reduction of GnRH in terms of both gene and

protein expression. These findings are consistent with previous studies reporting GnRH gene expression alteration in the mouse hypothalamic GT1-7 cell line exposed to other EDCs, such as polychlorinated biphenyls (Gore et al., 2002) and in *in vivo* studies in the sheep, where GnRH mRNA was decreased by the EDC bisphenol A (Mahoney and Padmanabhan, 2010).

At present, the main research in the field is focused on the effects of the most popular EDCs, such as bisphenol A at the hypothalamic level (Lopez-Rodriguez et al., 2020; Ruffinatti et al., 2019), whereas only few studies have investigated the action of BaP on GnRH neurons, despite in certain urban and industrial areas the population is dramatically exposed to this toxicant. In particular, studies on the effect of BaP exposure are just limited to few researches in teleosts. Consistent with our findings, Gao and co-workers reported a GnRH1 mRNA expression decrease, following long-term embryonic exposure to BaP in zebrafish, associated with *GnRH1* gene methylation (Gao et al., 2018). On the contrary, a recent study in lined *Hippocampus erectus* demonstrated an increase of GnRH1 transcript expression after short-term effect of BaP (Wang et al., 2019). Data from our previous report (Guarnieri et al., 2021) indicated no significant changes of GnRH1 mRNA expression in FNCB4. This apparent discrepancy may actually suggest the complexity of BaP effects, which could depend not only on the duration of the exposure, but also on the physiological state of the cell at the moment of the exposure. In particular, comparing the cellular models used in our previous study (Guarnieri et al., 2021) and in the present one, they are representative of different steps of GnRH neuronal maturation and therefore their responsiveness to BaP may be different. FNCB4, derived from the nasal placode, are representative of early steps of GnRH neurons maturation when the neuroblasts are mainly involved in cell migration regulatory pathways. GnRH expression and release could instead characterize more crucially the functional activity of post-migratory hfHypo cells in comparison to FNCB4.

Another interesting observation is that BaP exposure significantly reduced both gene and protein expression of KISS1R/GPR54 in hfHypo cells. It is well known that the kisspeptin/KISS1R system is crucially required as physiological regulator of mature hypothalamic GnRH neurons function, controlling GnRH neurons activation and GnRH peptide release (Tng, 2015). The inhibitory effect of BaP on KISS1R expression in hfHypo cells supports the hypothesis that the exposure to the pollutant may alter the physiological responsiveness of GnRH-secreting neurons to kisspeptin. Our results are consistent with data concerning other EDCs, such as phthalates, which showed mixed effects on KISS1R expression depending on dose, duration, and developmental period of exposures in a rat model (Graceli et al., 2020). However, to our knowledge, no further information is available on the effect of BaP on KISS1R expression in hypothalamic cells. In this context, our findings may help to clarify the mechanisms through which GnRH neurons responsiveness to kisspeptin could be altered by BaP exposure.

It is well documented that the administration of BaP resulted in a significant increase of pro-inflammatory cytokines, including TNFα (Adedara et al., 2015; Lou et al., 2022; Malik et al., 2018; Zheng et al., 2010). Previous research carried out in a rabbit model demonstrated that metabolic syndrome-related hypothalamic inflammation was associated with the GnRH neuron impairment and, consequently, reduction of gonadotropins and sex hormones levels (Morelli et al., 2014). In this rabbit model, the hypothalamic dysfunction evocated by a pro-inflammatory status was associated with a significant reduction of KISS1R positivity. Accordingly, we recently reported (Sarchielli et al., 2017) that TNFα directly affects hfHypo cells decreasing KISS1R mRNA level and downregulating kisspeptin signaling. Moreover, KISS1R mRNA was significantly reduced by BaP exposure in FNCB4 (Guarnieri et al., 2021). Overall, we could speculate that a possible mechanism through which BaP downregulates KISS1R in hfHypo cells may be related to the induction of a local proinflammatory microenvironment. Consistent with this hypothesis we found a significant increase of COX-2 mRNA level, a well-known inducible target by TNFα (Guarnieri et al., 2020), after BaP exposure of hfHypo cells, as also reported in rat astrocytes treated with BaP *in vivo* and *in vitro* (Weng, 2004). However, we did not demonstrate any induction of TNFα expression in hfHypo exposed to BaP, thus suggesting that different mechanisms, not TNFα-mediated, may activate the COX-2-related inflammatory signaling. In this regard, AhR activation could be involved, as reported previously (Degner et al., 2007; Guo et al., 2020).

In this study, we also demonstrated that exposing hfHypo cells to BaP determined a significant induction of ERK1/2 phosphorylation. This ability of BaP in exerting its effects has been well documented in previous studies (Sun et al., 2021; Vázquez-Gómez et al., 2018). Since KISS1R activation by kisspeptin also recruits pERK1/2 intracellular pathways (Szereszewski et al., 2010), we can hypothesize that this could be a mechanism through which BaP could interfere with KISS1R signaling. Indeed, kisspeptin was unable to further induce ERK1/2 phosphorylation in BaP-treated hfHypo cells, thus suggesting that GnRH neurons may be less sensitive to their physiological regulator in presence of BaP.

To further investigate the effect of BaP on GnRH neurons function we analyzed whether the downregulation of the expression of both GnRH and KISS1R was also related to alterations in GnRH-secreting ability of hfHypo cells. Surprisingly, we found that in the presence of BaP the amount of GnRH peptide released by the cells in the culture medium was significantly increased. This finding is apparently in contrast with the observation of a reduction in GnRH protein expression, in terms of both the number of GnRH-positive cells and total amount of GnRH protein. To explain this discrepancy, we hypothesized a dual mechanism of action through which BaP may affect not only the hfHypo phenotype (reduced GnRH and KISS1R expression), but also their functional properties increasing the GnRH-secreting ability. Accordingly, the BaP-mediated activation of GnRH release in the culture medium could contribute to the protein depletion within the cellular compartments, as detected by FACS. Consisting with this finding we observed that BaP was able to affect the hfHypo cell electrophysiological properties, causing a significant depolarization of the RMP. This effect could be responsible not only for the not-physiological release of GnRH by the cells, but also for the decreased response to the TRPC current-mediated depolarizing, and physiological, stimulus of kisspeptin, as expected by KISS1R activation (Kotani et al., 2001). The well-known ability of BaP, linked to its carcinogenic action, in altering the lipid profile and physiochemical property of membranes (Bhardwaj et al., 2019) is consistent with our results. However, further studies are needed to better characterize the BaP-induced mechanisms responsible for membrane depolarization in hfHypo cells.

We also found that BaP affected mRNA expression of hormone receptors, such as AR and GPER1, further confirming a role of the toxicant as EDCs. In particular, AR expression was reduced by BaP in hfHypo cells, consistent with previous several reports that have indicated that BaP (but also other PAHs acting as AhR ligands) may interfere with nuclear receptor activity, including AR (Lin et al., 2004; Šimečková et al., 2022). In contrast, the membrane estrogen receptor GPER1/GPR30, which has been implicated in rapid action of estrogen in GnRH neurons (Noel et al., 2009), was increased by BaP in hfHypo cells. A relation between the altered expression of AR and GPER1 and GnRH secretion has not been specifically investigated but merits to be addressed in future studies.

Taken together, our findings demonstrate for the first time in a human cellular model that BaP exposure may directly affect the normal physiology and function of GnRH-secreting neurons. By a mechanistic point of view, the effects of BaP on hfHypo cells may be summarized in 1) oxidative stress induction (ROS generation and activation of TAC); 2) AhR-mediated downstream effects, such as activation of inflammatory signaling (COX2 induction) and gene expression alteration (GnRH, KISS1R, sex hormone receptors) leading to phenotypic changes; 3) perturbations of membrane properties leading to membrane depolarization and changes in ionic currents. In particular, we can hypothesize

that the exposure to BaP may contribute to desensitize GnRH neurons to the physiological depolarizing stimulation of kisspeptin, which in turn may result in an uncontrolled functional activity in terms of GnRH secretion.

By a translational point of view, our study could support clinical reports that indicated how EDCs may anticipate the puberty onset (Parent et al., 2015) through a direct action on the HPG axis or indirectly on target organs, including adipose tissue or adrenal glands (Lee et al., 2019). Interestingly, it has been proposed that environmental pollutants can affect genes linked to HPG pathways, or alter metabolic programming during prenatal and early childhood development, interfering with the timing of puberty onset and fertility (Roth and DiVall, 2016). Epidemiologic data demonstrating a causal relationship between BaP exposure and changes in pubertal timing are still lacking. In this context, although being obtained *in vitro* and not complete in terms of mechanistic findings, our results may be regarded as a good proof of concept for encouraging future studies aimed at better clarifying the toxicity mechanisms of BaP on human GnRH neurons and thereby human reproduction.

5. Conclusions

In conclusion, we hereby provide the first evidence in a human *in vitro* model that BaP exposure may directly affect post-migratory GnRH neuron function by reducing GnRH and KISS1R expression, altering electrophysiological property, and interfering with kisspeptin/KISS1R signaling and GnRH secretion. Hence, our results identified a possible EDCs-related mechanism at central level underlying reproductive function alterations due to persistent exposure to environmental pollutants, such as BaP.

Funding

This study was supported by a grant from MUR (Ministero dell'Università e della Ricerca, Italy; MIUR-PRIN2017, grant no. 2017TK7Z8L_006).

Author contribution

GG, performed experiments, analyzed data, generated figures, and wrote the manuscript; MB, performed FACs analysis, contributed to experiments and interpretation of data; RS, contributed to electrophysiological experiments and interpretation of data; PC, contributed to gene expression experiments; RG, performed electrophysiological experiments; LT and SM revised the manuscript; LV, GBV, MM, helped for resources and revised the manuscript; AM, contributed to the conception and development of the project, data interpretation and wrote the manuscript. All authors have read and agreed to the published version of the manuscript.

Declaration of competing interest

The authors declare that they have no known competing financial interests or personal relationships that could have appeared to influence the work reported in this paper.

Data availability

Data will be made available on request.

Acknowledgments

The authors wish to thank Professor Emilia Rocco (Department of Statistics, Computer Science, Applications, University of Florence) for her assistance in the statistical analysis.

References

Adedara, I.A., Owoeye, O., Aiyegbusi, M.A., Dagunduro, J.O., Daramola, Y.M., Farombi, E.O., 2015. Kolaviron protects against benzo[a]pyrene-induced functional alterations along the brain-pituitary-gonadal axis in male rats. Environ. Toxicol. Pharmacol. 40, 459–470. https://doi.org/10.1016/j.etap.2015.07.015.

Alamo, A., Condorelli, R.A., Mongioì, L.M., Cannarella, R., Giacone, F., Calabrese, V., La Vignera, S., Calogero, A.E., 2019. Environment and male fertility: effects of benzo-α-pyrene and resveratrol on human sperm function in vitro. J. Clin. Med. 8, 561. https://doi.org/10.3390/jcm8040561.

Alegbeleye, O.O., Opeolu, B.O., Jackson, V.A., 2017. Polycyclic aromatic hydrocarbons: a critical review of environmental occurrence and bioremediation. Environ. Manag. 60, 758–783. https://doi.org/10.1007/s00267-017-0896-2.

Becatti, M., Fucci, R., Mannucci, A., Barygina, V., Mugnaini, M., Criscuoli, L., Giachini, C., Bertocci, F., Picone, R., Emmi, G., Evangelisti, P., Rizzello, F., Cozzi, C., Taddei, N., Fiorillo, C., Coccia, M.E., 2018. A biochemical approach to detect oxidative stress in infertile women undergoing assisted reproductive Technology procedures. IJMS 15, 592.

Becatti, M., Marcucci, R., Gori, A.M., Mannini, L., Grifoni, E., Alessandrello Liotta, A., Sodi, A., Tartaro, R., Taddei, N., Rizzo, S., Prisco, D., Abbate, R., Fiorillo, C., 2016. Erythrocyte oxidative stress is associated with cell deformability in patients with retinal vein occlusion. J. Thromb. Haemostasis 14, 2287–2297. https://doi.org/10.1111/jth.13482.

Bhardwaj, P., Kumar, M., Dhatwalia, S.K., Garg, M.L., Dhawan, D.K., 2019. Acetyl-11-keto-β-boswellic acid modulates membrane dynamics in benzo(a)pyrene-induced lung carcinogenesis. Mol. Cell. Biochem. 460, 17–27. https://doi.org/10.1007/s11010-019-03566-z.

Bloch, B., Gaillard, R.C., Culler, M.D., Negro-Vilar, A., 1992. Immunohistochemical detection of proluteinizing hormone-releasing hormone peptides in neurons in the human hypothalamus. J. Clin. Endocrinol. Metab. 74, 135–138. https://doi.org/10.1210/jcem.74.1.1727812.

Bolden, A.L., Rochester, J.R., Schultz, K., Kwiatkowski, C.F., 2017. Polycyclic aromatic hydrocarbons and female reproductive health: a scoping review. Reprod. Toxicol. 73, 61–74. https://doi.org/10.1016/j.reprotox.2017.07.012.

Bukowska, B., Mokra, K., Michałowicz, J., 2022. Benzo[a]pyrene—environmental occurrence, human exposure, and mechanisms of toxicity. IJMS 23, 6348. https://doi.org/10.3390/ijms23116348.

Casoni, F., Malone, S.A., Belle, M., Luzzati, F., Collier, F., Allet, C., Hrabovszky, E., Rasika, S., Prevot, V., Chédotal, A., Giacobini, P., 2016. Development of the neurons controlling fertility in humans: new insights from 3D imaging and transparent fetal brains. Development 143, 3969–3981. https://doi.org/10.1242/dev.139444.

Chen, C., Tang, Y., Jiang, X., Qi, Y., Cheng, S., Qiu, C., Peng, B., Tu, B., 2012. Early postnatal benzo(a)pyrene exposure in sprague-dawley rats causes persistent neurobehavioral impairments that emerge postnatally and continue into adolescence and adulthood. Toxicol. Sci. 125, 248–261. https://doi.org/10.1093/toxsci/kfr265.

Chiba, T., Uchi, H., Tsuji, G., Gondo, H., Moroi, Y., Furue, M., 2011. Arylhydrocarbon receptor (AhR) activation in airway epithelial cells induces MUC5AC via reactive oxygen species (ROS) production. Pulm. Pharmacol. Ther. 24, 133–140. https://doi.org/10.1016/j.pupt.2010.08.002.

Das, M., Seth, P.K., Mukhtar, H., 1985. Distribution of benzo(a)pyrene in discrete regions of rat brain. Bull. Environ. Contam. Toxicol. 35, 500–504. https://doi.org/10.1007/BF01636545.

Degner, S.C., Kemp, M.Q., Hockings, J.K., Romagnolo, D.F., 2007. Cyclooxygenase-2 promoter activation by the aromatic hydrocarbon receptor in breast cancer MCF-7 cells: repressive effects of conjugated linoleic acid. Nutr. Cancer 59, 248–257. https://doi.org/10.1080/01635580701485585.

Dong, Q., Hou, H., Wu, J., Chen, Y., 2016. The Nrf 2-ARE pathway is associated with Schisandrin b attenuating benzo(a)pyrene-Induced HTR cells damages *in vitro*: schisandrin b attenuating benzo(a)pyrene-induced HTR cells. Environ. Toxicol. 31, 1439–1449. https://doi.org/10.1002/tox.22149.

Einaudi, L., Courbiere, B., Tassistro, V., Prevot, C., Sari-Minodier, I., Orsiere, T., Perrin, J., 2014. In vivo exposure to benzo(a)pyrene induces significant DNA damage in mouse oocytes and cumulus cells. Hum. Reprod. 29, 548–554. https://doi.org/10.1093/humrep/det439.

Formigli, L., Sassoli, C., Squecco, R., Bini, F., Martinesi, M., Chellini, F., Luciani, G., Sbrana, F., Zecchi-Orlandini, S., Francini, F., Meacci, E., 2009. Regulation of transient receptor potential canonical channel 1 (TRPC1) by sphingosine 1-phosphate in C2C12 myoblasts and its relevance for a role of mechanotransduction in skeletal muscle differentiation. J. Cell Sci. 122, 1322–1333. https://doi.org/10.1242/jcs.035402.

Gao, D., Lin, J., Ou, K., Chen, Y., Li, H., Dai, Q., Yu, Z., Zuo, Z., Wang, C., 2018. Embryonic exposure to benzo(a)pyrene inhibits reproductive capability in adult female zebrafish and correlation with DNA methylation. Environ. Pollut. 240, 403–411. https://doi.org/10.1016/j.envpol.2018.04.139.

Gelboin, H.V., 1980. Benzo[alpha]pyrene metabolism, activation and carcinogenesis: role and regulation of mixed-function oxidases and related enzymes. Physiol. Rev. 60, 1107–1166. https://doi.org/10.1152/physrev.1980.60.4.1107.

Gore, A.C., Chappell, V.A., Fenton, S.E., Flaws, J.A., Nadal, A., Prins, G.S., Toppari, J., Zoeller, R.T., 2015. EDC-2: the endocrine society's second scientific statement on endocrine-disrupting chemicals. Endocr. Rev. 36, E1–E150. https://doi.org/10.1210/er.2015-1010.

Gore, A.C., Wu, T.J., Oung, T., Lee, J.B., Woller, M.J., 2002. A novel mechanism for endocrine-disrupting effects of polychlorinated biphenyls: direct effects on gonadotropin-releasing hormone neurones: PCBs and GnRH neurones. J. Neuroendocrinol. 14, 814–823. https://doi.org/10.1046/j.1365-2826.2002.00845.x.

Graceli, J.B., Dettogni, R.S., Merlo, E., Niño, O., da Costa, C.S., Zanol, J.F., Ríos Morris, E. A., Miranda-Alves, L., Denicol, A.C., 2020. The impact of endocrine-disrupting chemical exposure in the mammalian hypothalamic-pituitary axis. Mol. Cell. Endocrinol. 518, 110997 https://doi.org/10.1016/j.mce.2020.110997.

Guarnieri, G., Becatti, M., Comeglio, P., Vignozzi, L., Maggi, M., Vannelli, G.B., Morelli, A., 2021. Benzo[a]pyrene impairs the migratory pattern of human gonadotropin-releasing-hormone-secreting neuroblasts. Eur. J. Histochem. 65 https://doi.org/10.4081/ejh.2021.3282.

Guarnieri, G., Sarchielli, E., Comeglio, P., Herrera-Puerta, E., Piaceri, I., Nacmias, B., Benelli, M., Kelsey, G., Maggi, M., Gallina, P., Vannelli, G.B., Morelli, A., 2020. Tumor necrosis factor α influences phenotypic plasticity and promotes epigenetic changes in human basal forebrain cholinergic neuroblasts. IJMS 21, 6128. https://doi.org/10.3390/ijms21176128.

Guo, L., Wei, M., Li, B., Yun, Y., Li, G., Sang, N., 2020. The role of cyclooxygenases-2 in benzo(*a*)pyrene-Induced neurotoxicity of cortical neurons. Chem. Res. Toxicol. 33, 1364–1373. https://doi.org/10.1021/acs.chemrestox.9b00451.

Herde, M.K., Geist, K., Campbell, R.E., Herbison, A.E., 2011. Gonadotropin-releasing hormone neurons extend complex highly branched dendritic trees outside the blood-brain barrier. Endocrinology 152, 3832–3841. https://doi.org/10.1210/en.2011-1228.

Hsu, P.-C., Chen, I.-Y., Pan, C.-H., Wu, K.-Y., Pan, M.-H., Chen, J.-R., Chen, C.-J., Chang-Chien, G.-P., Hsu, C.-H., Liu, C.-S., Wu, M.-T., 2006. Sperm DNA damage correlates with polycyclic aromatic hydrocarbons biomarker in coke-oven workers. Int. Arch. Occup. Environ. Health 79, 349–356. https://doi.org/10.1007/s00420-005-0066-3.

Inyang, F., 2003. Disruption of testicular steroidogenesis and epididymal function by inhaled benzo(a)pyrene. Reprod. Toxicol. 17, 527–537. https://doi.org/10.1016/S0890-6238(03)00071-6.

Jeng, H.A., Pan, C.-H., Chao, M.-R., 2013. 1-Hydroxypyrene as a biomarker for assessing the effects of exposure to polycyclic aromatic hydrocarbons on semen quality and sperm DNA integrity. J. Environ. Sci. Health, Part A: Toxic/Hazard. Subst. Environ. Eng. 48, 152–158. https://doi.org/10.1080/03601234.2012.716741.

Ji, K., Xing, C., Jiang, F., Wang, X., Guo, H., Nan, J., Qian, L., Yang, P., Lin, J., Li, M., Li, J., Liao, L., Tang, J., 2013. Benzo[a]pyrene induces oxidative stress and endothelial progenitor cell dysfunction via the activation of the NF-κB pathway. Int. J. Mol. Med. 31, 922–930. https://doi.org/10.3892/ijmm.2013.1288.

Kanaly, R.A., Harayama, S., 2000. Biodegradation of high-molecular-weight polycyclic aromatic hydrocarbons by bacteria. J. Bacteriol. 182, 2059–2067. https://doi.org/10.1128/JB.182.8.2059-2067.2000.

Kotani, M., Detheux, M., Vandenbogaerde, A., Communi, D., Vanderwinden, J.-M., Le Poul, E., Brézillon, S., Tyldesley, R., Suarez-Huerta, N., Vandeput, F., Blanpain, C., Schiffmann, S.N., Vassart, G., Parmentier, M., 2001. The metastasis suppressor gene KiSS-1 encodes kisspeptins, the natural ligands of the orphan G protein-coupled receptor GPR54. J. Biol. Chem. 276, 34631–34636. https://doi.org/10.1074/jbc.M104847200.

Lee, J.E., Jung, H.W., Lee, Y.J., Lee, Y.A., 2019. Early-life exposure to endocrine-disrupting chemicals and pubertal development in girls. Ann. Pediatr. Endocrinol,. Metab. 24, 78–91. https://doi.org/10.6065/apem.2019.24.2.78.

Lin, P., Chang, J.T., Ko, J.-L., Liao, S.-H., Lo, W.-S., 2004. Reduction of androgen receptor expression by benzo[a]pyrene and 7,8-dihydro-9,10-epoxy-7,8,9,10-tetrahydro-benzo[a]pyrene in human lung cells. Biochem. Pharmacol. 67, 1523–1530. https://doi.org/10.1016/j.bcp.2003.12.018.

Liu, D., Zhao, Y., Qi, Y., Gao, Y., Tu, D., Wang, Y., Gao, H.-M., Zhou, H., 2020. Benzo(a) pyrene exposure induced neuronal loss, plaque deposition, and cognitive decline in APP/PS1 mice. J. Neuroinflammation 17, 258. https://doi.org/10.1186/s12974-020-01925-y.

Livak, K.J., Schmittgen, T.D., 2001. Analysis of relative gene expression data using real-time quantitative PCR and the 2−ΔΔCT method. Methods 25, 402–408. https://doi.org/10.1006/meth.2001.1262.

Lopez-Rodriguez, D., Franssen, D., Bakker, J., Lomniczi, A., Parent, A.-S., 2020. Cellular and molecular features of EDC exposure: consequences for the GnRH network. Nat. Rev. Endocrinol. https://doi.org/10.1038/s41574-020-00436-3.

Lou, W., Zhang, M., Chen, Q., Bai, T.-Y., Hu, Y.-X., Gao, F., Li, J., Lv, X.-L., Zhang, Q., Chang, F.-H., 2022. Molecular mechanism of benzo [a] pyrene regulating lipid metabolism via aryl hydrocarbon receptor. Lipids Health Dis. 21, 13. https://doi.org/10.1186/s12944-022-01627-9.

Mahoney, M.M., Padmanabhan, V., 2010. Developmental programming: impact of fetal exposure to endocrine-disrupting chemicals on gonadotropin-releasing hormone and estrogen receptor mRNA in sheep hypothalamus. Toxicol. Appl. Pharmacol. 247, 98–104. https://doi.org/10.1016/j.taap.2010.05.017.

Malik, D., David, R.M., Gooderham, N.J., 2018. Mechanistic evidence that benzo[a] pyrene promotes an inflammatory microenvironment that drives the metastatic potential of human mammary cells. Arch. Toxicol. 92, 3223–3239. https://doi.org/10.1007/s00204-018-2291-z.

Mansuy, V., Geller, S., Rey, J.-P., Campagne, C., Boccard, J., Poulain, P., Prevot, V., Pralong, F.P., 2011. Phenotypic and molecular characterization of proliferating and differentiated GnRH-expressing GnV-3 cells. Mol. Cell. Endocrinol. 332, 97–105. https://doi.org/10.1016/j.mce.2010.10.001.

Marraudino, M., Bonaldo, B., Farinetti, A., Panzica, G., Ponti, G., Gotti, S., 2019. Metabolism disrupting chemicals and alteration of neuroendocrine circuits controlling food intake and energy metabolism. Front. Endocrinol. 9, 766. https://doi.org/10.3389/fendo.2018.00766.

Mellon, P.L., Goldsmith, P.C., Padula, C.A., Roberts, J.L., Weiner, R.I., 1990. Immortalization of hypothalamic GnRH neurons by genetically targeted tumorigenesis. Neuron 5, 1–10. https://doi.org/10.1016/0896-6273(90)90028-e.

Mohamed, E.-S.A., Song, W.-H., Oh, S.-A., Park, Y.-J., You, Y.-A., Lee, S., Choi, J.-Y., Kim, Y.-J., Jo, I., Pang, M.-G., 2010. The transgenerational impact of benzo(a)pyrene on murine male fertility. Hum. Reprod. 25, 2427–2433. https://doi.org/10.1093/humrep/deq205.

Moreira, P.I., Zhu, X., Liu, Q., Honda, K., Siedlak, S.L., Harris, P.L., Smith, M.A., Perry, G., 2006. Compensatory responses induced by oxidative stress in Alzheimer disease. Biol. Res. 39 https://doi.org/10.4067/S0716-97602006000100002.

Morelli, A., Marini, M., Mancina, R., Luconi, M., Vignozzi, L., Fibbi, B., Filippi, S., Pezzatini, A., Forti, G., Vannelli, G.B., Maggi, M., 2008. Sex steroids and leptin regulate the "first kiss" (KiSS 1/G-protein-coupled receptor 54 system) in human gonadotropin-releasing-hormone-secreting neuroblasts. J. Sex. Med. 5, 1097–1113. https://doi.org/10.1111/j.1743-6109.2008.00782.x.

Morelli, A., Sarchielli, E., Comeglio, P., Filippi, S., Vignozzi, L., Marini, M., Rastrelli, G., Maneschi, E., Cellai, I., Persani, L., Adorini, L., Vannelli, G.B., Maggi, M., 2014. Metabolic syndrome induces inflammation and impairs gonadotropin-releasing hormone neurons in the preoptic area of the hypothalamus in rabbits. Mol. Cell. Endocrinol. 382, 107–119. https://doi.org/10.1016/j.mce.2013.09.017.

Neal, M.S., Zhu, J., Holloway, A.C., Foster, W.G., 2007. Follicle growth is inhibited by benzo-[a]-pyrene, at concentrations representative of human exposure, in an isolated rat follicle culture assay. Hum. Reprod. 22, 961–967. https://doi.org/10.1093/humrep/del487.

Netter, A., Siri, E., Tassitro, V., Resseguier, N., Beauval, N., Sari-Minodier, I., Courbiere, B., Perrin, J., 2020. Influence of polycyclic aromatic hydrocarbon exposure on IVF: now is the time to focus on women. Reprod. Biomed. Online 41, 161–169. https://doi.org/10.1016/j.rbmo.2020.03.022.

Nguyen, P.M., Park, M.S., Chow, M., Chang, J.H., Wrischnik, L., Chan, W.K., 2010. Benzo [a]pyrene increases the Nrf 2 content by downregulating the Keap 1 message. Toxicol. Sci. 116, 549–561. https://doi.org/10.1093/toxsci/kfq150.

Niu, Q., Zhang, H., Li, X., Li, M., 2010. Benzo[a]pyrene-induced neurobehavioral function and neurotransmitter alterations in coke oven workers. Occup. Environ. Med. 67, 444. https://doi.org/10.1136/oem.2009.047969.

Noel, S.D., Keen, K.L., Baumann, D.I., Filardo, E.J., Terasawa, E., 2009. Involvement of G Protein-Coupled receptor 30 (GPR30) in rapid action of estrogen in primate LHRH neurons. Mol. Endocrinol. 23, 349–359. https://doi.org/10.1210/me.2008-0299.

Parent, A.-S., Franssen, D., Fudvoye, J., Gérard, A., Bourguignon, J.-P., 2015. Developmental variations in environmental influences including endocrine disruptors on pubertal timing and neuroendocrine control: revision of human observations and mechanistic insight from rodents. Front. Neuroendocrinol. 38, 12–36. https://doi.org/10.1016/j.yfrne.2014.12.004.

Pensalfini, A., Cecchi, C., Zampagni, M., Becatti, M., Favilli, F., Paoli, P., Catarzi, S., Bagnoli, S., Nacmias, B., Sorbi, S., Liguri, G., 2008. Protective effect of new S-acylglutathione derivatives against amyloid-induced oxidative stress. Free Radic. Biol. Med. 44, 1624–1636. https://doi.org/10.1016/j.freeradbiomed.2008.01.025.

Pieterse, B., Felzel, E., Winter, R., van der Burg, B., Brouwer, A., 2013. PAH-CALUX, an optimized bioassay for AhR-mediated hazard identification of polycyclic aromatic hydrocarbons (PAHs) as individual compounds and in complex mixtures. Environ. Sci. Technol. 47, 11651–11659. https://doi.org/10.1021/es403810w.

Radovick, S., Wray, S., Lee, E., Nicols, D.K., Nakayama, Y., Weintraub, B.D., Westphal, H., Cutler, G.B., Wondisford, F.E., 1991. Migratory arrest of gonadotropin-releasing hormone neurons in transgenic mice. Proc. Natl. Acad. Sci. USA 88, 3402–3406. https://doi.org/10.1073/pnas.88.8.3402.

Ramesh, A., Archibong, A.E., Niaz, M.S., 2010. Ovarian susceptibility to benzo[a]Pyrene: tissue burden of metabolites and DNA adducts in F-344 rats. J. Toxicol. Environ. Health, Part A 73, 1611–1625. https://doi.org/10.1080/15287394.2010.514225.

Revel, A., Raanani, H., Younglai, E., Xu, J., Han, R., Savouret, J.-F., Casper, R.F., 2001. Resveratrol, a natural aryl hydrocarbon receptor antagonist, protects sperm from DNA damage and apoptosis caused by benzo(a)pyrene. Reprod. Toxicol. 15, 479–486. https://doi.org/10.1016/S0890-6238(01)00149-6.

Rønnekleiv, O.K., Kelly, M.J., 2013. Kisspeptin excitation of GnRH neurons. In: Kauffman, A.S., Smith, J.T. (Eds.), Kisspeptin Signaling in Reproductive Biology, Advances in Experimental Medicine and Biology. Springer New York, New York, NY, pp. 113–131. https://doi.org/10.1007/978-1-4614-6199-9_6.

Roth, C.L., DiVall, S., 2016. Consequences of early life programing by genetic and environmental influences: a synthesis regarding pubertal timing. In: Bourguignon, J.-P., Parent, A.-S. (Eds.), Endocrine Development. S. Karger AG, pp. 134–152. https://doi.org/10.1159/000438883.

Ruffinatti, F.A., Gilardino, A., Secchi, V., Cottone, E., Lovisolo, D., Bovolin, P., 2019. Bisphenol A activates calcium influx in immortalized GnRH neurons. IJMS 20, 2160. https://doi.org/10.3390/ijms20092160.

Saha, S., Mahapatra, K.K., Mishra, S.R., Mallick, S., Negi, V.D., Sarangi, I., Patil, S., Patra, S.K., Bhutia, S.K., 2020. Bacopa monnieri inhibits apoptosis and senescence through mitophagy in human astrocytes. Food Chem. Toxicol. 141, 111367 https://doi.org/10.1016/j.fct.2020.111367.

Sarchielli, E., Comeglio, P., Squecco, R., Ballerini, L., Mello, T., Guarnieri, G., Idrizaj, E., Mazzanti, B., Vignozzi, L., Gallina, P., Maggi, M., Vannelli, G.B., Morelli, A., 2017. Tumor necrosis factor α impairs kisspeptin signaling in human gonadotropin-releasing hormone primary neurons. J. Clin. Endocrinol. Metab. jc 2016–2115. https://doi.org/10.1210/jc.2016-2115.

Sarchielli, E., Morelli, A., Guarnieri, G., Iorizzi, M., Sgambati, E., 2018. Neuroprotective effects of quercetin 4'- O -β- d -diglucoside on human striatal precursor cells in nutrient deprivation condition. Acta Histochem. 120, 122–128. https://doi.org/10.1016/j.acthis.2018.01.003.

Sarma, S.N., Blais, J.M., Chan, H.M., 2017. Neurotoxicity of alkylated polycyclic aromatic compounds in human neuroblastoma cells. J. Toxicol. Environ. Health, Part A 80, 285–300. https://doi.org/10.1080/15287394.2017.1314840.

Saunders, C.R., Das, S.K., Ramesh, A., Shockley, D.C., Mukherjee, S., 2006. Benzo(a) pyrene-induced acute neurotoxicity in the F-344 rat: role of oxidative stress. J. Appl. Toxicol. 26, 427–438. https://doi.org/10.1002/jat.1157.

Saunders, C.R., Shockley, D.C., Knuckles, M.E., 2001. Behavioral effects induced by acute exposure to benzo(a)pyrene in F-344 rats. Neurotox. Res. 3, 557–579. https://doi.org/10.1007/BF03033211.

Schiering, C., Wincent, E., Metidji, A., Iseppon, A., Li, Y., Potocnik, A.J., Omenetti, S., Henderson, C.J., Wolf, C.R., Nebert, D.W., Stockinger, B., 2017. Feedback control of AHR signalling regulates intestinal immunity. Nature 542, 242–245. https://doi.org/10.1038/nature21080.

Schwanzel-Fukuda, M., Crossin, K.L., Pfaff, D.W., Bouloux, P.M.G., 1996. Migration of luteinizing hormone—releasing hormone (LHRH) neurons in early human embryos. J. Comp. Neurol. 366, 547–557.

Segal, T.R., Giudice, L.C., 2019. Before the beginning: environmental exposures and reproductive and obstetrical outcomes. Fertil. Steril. 112, 613–621. https://doi.org/10.1016/j.fertnstert.2019.08.001.

Šimečková, P., Pěnčíková, K., Kováč, O., Slavík, J., Pařenicová, M., Vondráček, J., Machala, M., 2022. In vitro profiling of toxic effects of environmental polycyclic aromatic hydrocarbons on nuclear receptor signaling, disruption of endogenous metabolism and induction of cellular stress. Sci. Total Environ. 815, 151967 https://doi.org/10.1016/j.scitotenv.2021.151967.

Slotkin, T.A., Card, J., Seidler, F.J., 2013. Adverse benzo[*a*]pyrene effects on neurodifferentiation are altered by other neurotoxicant coexposures: interactions with dexamethasone, chlorpyrifos, or nicotine in PC12 cells. Environ. Health Perspect. 121, 825–831. https://doi.org/10.1289/ehp.1306528.

Slotkin, T.A., Seidler, F.J., 2009. Benzo[a]pyrene impairs neurodifferentiation in PC12 cells. Brain Res. Bull. 80, 17–21. https://doi.org/10.1016/j.brainresbull.2009.06.003.

Soares, S.R., Melo, M.A., 2008. Cigarette smoking and reproductive function. Curr. Opin. Obstet. Gynecol. 20, 281–291. https://doi.org/10.1097/GCO.0b013e3282fc9c1e.

Squecco, R., Sassoli, C., Garella, R., Chellini, F., Idrizaj, E., Nistri, S., Formigli, L., Bani, D., Francini, F., 2015. Inhibitory effects of relaxin on cardiac fibroblast-to-myofibroblast transition: an electrophysiological study: relaxin inhibits cardiac myofibroblast differentiation. Exp. Physiol. 100, 652–666. https://doi.org/10.1113/EP085178.

Street, M., Angelini, S., Bernasconi, S., Burgio, E., Cassio, A., Catellani, C., Cirillo, F., Deodati, A., Fabbrizi, E., Fanos, V., Gargano, G., Grossi, E., Iughetti, L., Lazzeroni, P., Mantovani, A., Migliore, L., Palanza, P., Panzica, G., Papini, A., Parmigiani, S., Predieri, B., Sartori, C., Tridenti, G., Amarri, S., 2018. Current knowledge on endocrine disrupting chemicals (EDCs) from animal biology to humans, from pregnancy to adulthood: highlights from a national Italian meeting. IJMS 19, 1647. https://doi.org/10.3390/ijms19061647.

Sun, Y., Shi, Z., Lin, Y., Zhang, M., Liu, J., Zhu, L., Chen, Q., Bi, J., Li, S., Ni, Z., Wang, X., 2021. Benzo(a)pyrene induces MUC5AC expression through the AhR/mitochondrial ROS/ERK pathway in airway epithelial cells. Ecotoxicol. Environ. Saf. 210, 111857 https://doi.org/10.1016/j.ecoenv.2020.111857.

Szereszewski, J.M., Pampillo, M., Ahow, M.R., Offermanns, S., Bhattacharya, M., Babwah, A.V., 2010. GPR54 regulates ERK1/2 activity and hypothalamic gene expression in a gαq/11 and β-arrestin-dependent manner. PLoS One 5, e12964. https://doi.org/10.1371/journal.pone.0012964.

Tng, E., 2015. Kisspeptin signalling and its roles in humans. Singap. Med. J. 56, 649–656. https://doi.org/10.11622/smedj.2015183.

Uppstad, H., Øvrebø, S., Haugen, A., Mollerup, S., 2010. Importance of CYP1A1 and CYP1B1 in bioactivation of benzo[a]pyrene in human lung cell lines. Toxicol. Lett. 192, 221–228. https://doi.org/10.1016/j.toxlet.2009.10.025.

Vázquez-Gómez, G., Rocha-Zavaleta, L., Rodríguez-Sosa, M., Petrosyan, P., Rubio-Lightbourn, J., 2018. Benzo[a]pyrene activates an AhR/Src/ERK axis that contributes to CYP1A1 induction and stable DNA adducts formation in lung cells. Toxicol. Lett. 289, 54–62. https://doi.org/10.1016/j.toxlet.2018.03.012.

Wang, W., Chen, J., Fang, Y., Wang, B., Zou, Q., Wang, L., Zhang, W., Huang, X., Lv, H., Zhang, C., Wang, K., 2019. Identification of gnrh2 and gnrh3 and their expression during brood pouch growth and short-term benzo(a)pyrene exposure in lined seahorse (Hippocampus erectus). Comp. Biochem. Physiol. C Toxicol. Pharmacol. 225, 108579 https://doi.org/10.1016/j.cbpc.2019.108579.

Weng, M., 2004. Benzo6a9pyrene diol epoxide up-regulates COX-2 expression through NF-$kappa;B in rat astrocytes. Toxicol. Lett. 151, 345–355. https://doi.org/10.1016/j.toxlet.2004.03.007.

Whittaker, A., Sofi, F., Luisi, M., Rafanelli, E., Fiorillo, C., Becatti, M., Abbate, R., Casini, A., Gensini, G., Benedettelli, S., 2015. An organic khorasan wheat-based replacement diet improves risk profile of patients with acute coronary syndrome: a randomized crossover trial. Nutrients 7, 3401–3415. https://doi.org/10.3390/nu7053401.

Wray, S., 2010. From nose to brain: development of gonadotrophin-releasing hormone -1 neurones: GnRH development. J. Neuroendocrinol. 22, 743–753. https://doi.org/10.1111/j.1365-2826.2010.02034.x.

Zhang, C., Roepke, T.A., Kelly, M.J., Ronnekleiv, O.K., 2008. Kisspeptin depolarizes gonadotropin-releasing hormone neurons through activation of TRPC-like cationic channels. J. Neurosci. 28, 4423–4434. https://doi.org/10.1523/JNEUROSCI.5352-07.2008.

Zhang, L., Ji, X., Ding, F., Wu, X., Tang, N., Wu, Q., 2022. Apoptosis and blood-testis barrier disruption during male reproductive dysfunction induced by PAHs of different molecular weights. Environ. Pollut. 300, 118959 https://doi.org/10.1016/j.envpol.2022.118959.

Zheng, S., Tian, H., Cao, J., Gao, Y., 2010. Exposure to di(n-butyl)phthalate and benzo(a)pyrene alters IL-1β secretion and subset expression of testicular macrophages, resulting in decreased testosterone production in rats. Toxicol. Appl. Pharmacol. 248, 28–37. https://doi.org/10.1016/j.taap.2010.07.008.